Statistical Failure Analysis of Hybrid Bus Batteries: Using A Three-Year Maintenance Dataset from King County

Babita Giri

A thesis
submitted in partial fulfilment of the
requirements for the degree of

Master of Science

University of Washington

2025

Committee:

Daniel T Schwartz

Eric M Stuve

Program Authorized to Offer Degree:
Chemical Engineering

University of Washington

Abstract

Statistical Failure Analysis of Hybrid Bus Batteries: Using A Three-Year Maintenance Dataset from King County

Babita Giri

Chair of the Supervisory Committee:
Daniel T. Schwartz
Department of Chemical Engineering

This study introduces a data-driven framework for analyzing battery module failure patterns in hybrid-electric buses, with the goal of optimizing maintenance strategies and enhancing operational reliability. Buses are categorized as *Healthy* or *Swapped* based on historical maintenance frequency. Failure times are statistically modeled using Weibull and Gaussian distributions to identify dominant trends. Key reliability metrics—including mean time to failure (MTTF), standard deviation, R^2 values, KS-Statistic & p-value, and mean absolute error (MAE)—are employed to assess distribution fits at both fleet and module levels.

To investigate the root causes of premature failures, voltage data from more than 50,000 submodules are analyzed in time-binned intervals and correlated with documented failure events. Preliminary results reveal potential voltage-related degradation mechanisms, providing actionable insights for predictive maintenance. Ongoing research expands these analyses to higher-order modules, refining predictive models and generalizing findings across the fleet.

TABLE OF CONTENTS

LIST OF FIGURES

LIST OF TABLES

ACKNOWLEDGEMENT

I am deeply grateful to Professor Daniel T. Schwartz for his invaluable guidance, unwavering support, and mentorship throughout this research. His profound expertise, insightful feedback, and constant encouragement were pivotal to both the success of this work and my development as a researcher.

Chapter 1: Introduction

The rapid adoption of hybrid-electric buses in urban transit networks represents a critical step toward reducing greenhouse gas emissions and improving energy efficiency in public transportation [1]. These vehicles rely on sophisticated battery systems to perform two essential functions: providing high-power bursts for acceleration and capturing kinetic energy through regenerative braking [2]. Unlike conventional diesel buses, hybrid systems subject their battery packs to extreme and frequent charge-discharge cycles, creating unique maintenance challenges that transit agencies must address to ensure fleet reliability and cost-effectiveness [3,4].

Battery Fundamentals in Hybrid Transit Applications

Modern hybrid buses utilize nickel-metal hydride (NiMH) or lithium-ion (Li-ion) battery packs composed of multiple modules, each containing numerous individual cells [5]. These energy storage systems operate under demanding conditions, with design loads typically rated for peak power delivery during acceleration (often exceeding 100 kW), rapid charge acceptance during braking events, and continuous cycling in variable temperature environments [5]. The battery management system (BMS) continuously monitors key parameters, including voltage, current, temperature, and state of charge (SoC), to ensure safe operation [4]. However, even with proper management, batteries inevitably degrade through two primary mechanisms: capacity fade (reduction in energy storage capability) and power fade (decreased ability to deliver high currents). These unique operational profiles create maintenance challenges that transit agencies must proactively address through advanced monitoring, adaptive charging strategies, and predictive maintenance protocols. Failure to do so can lead to premature battery replacement costs (often 10,000–10,000–20,000 per pack) and unexpected vehicle downtime—undermining both the economic and environmental benefits of hybrid fleets [6,7]

Quantifying Battery Health and Performance

To quantify battery health and performance, transit agencies typically monitor two critical metrics: State of Health (SoH) and State of Function (SoF). SoH measures remaining energy capacity relative to the battery's original specification, with industry standards often considering batteries degraded when SoH falls below 80%. SoF assesses the battery's power capability, particularly its ability to meet the high-current demands of acceleration and regenerative braking [8].

Current maintenance practices, such as those employed by King County Metro, primarily rely on voltage dwell time - the duration a battery module spends below a predetermined voltage threshold - as a proxy for these health indicators. While this method provides a simple operational metric, it fails to capitalize on the wealth of additional data available from the BMS, potentially missing early warning signs of degradation [9].

Battery Degradation Mechanisms and Failure Modes

The complex architecture of hybrid bus battery systems introduces multiple potential failure points across different levels of the system. At the cell level, individual battery cells may degrade due to electrolyte decomposition, electrode material cracking, or separator breakdown, leading to increased internal resistance and reduced capacity over time [10]. These microscopic changes accumulate, ultimately impairing performance. On a larger scale, modules—composed of multiple interconnected cells—can experience imbalances, loose or corroded electrical connections, or localized overheating, which further accelerates deterioration. At the pack level, broader system failures may occur, including cooling system malfunctions, voltage imbalances between modules, or battery management system (BMS) errors[4]. Each of these failure modes contributes to overall battery degradation, impacting the reliability and efficiency of hybrid-electric buses in transit operations [11,12].

Research Objectives and Paper Organization

a) Scope of the Study

This study addresses critical challenges in battery degradation within hybrid-electric transit systems, with a specific focus on the battery modules used in King County Metro's (KCM) fleet of BAE Systems HybriDrive buses. As one of North America's largest hybrid bus operators, KCM offers an ideal case study, particularly with its fleet of approximately 200 vehicles acquired in 2010 that remain in active service. Each bus is equipped with a 12-kWh battery system consisting of 16 modules, each containing 12 series-connected submodules. These submodules are further composed of eight parallel-connected 2.3 Ah lithium iron phosphate ($LiFePO_4$) cells, forming a complex electrochemical system subjected to rigorous urban transit duty cycles [13].

The scale of this deployment—over 30,000 individual battery submodules in daily operation—makes effective degradation monitoring not only theoretically significant but also operationally essential. Currently, like most transit agencies, KCM relies on voltage-based health indicators, which may fail to detect early-stage capacity fade or reduced power capability. This limitation is particularly concerning given that the 2010-vintage batteries have now exceeded their typical 8–10-year design lifespan, replacement costs remain high (approximately $15,000 per module), and premature replacements strain maintenance budgets and disrupt service [13-15].

b) Research Objectives

This study aims to develop advanced battery health monitoring strategies by analyzing a three-year batteries maintenance dataset from KCM's HybriDrive buses. Focusing on the fleet's 12 kWh $LiFePO_4$ battery systems, the research will characterize degradation patterns by correlating key metrics such as mean time to failure and voltage dwell time with multidimensional operational data, including voltage profiles, temperature fluctuations, and charge/discharge cycles. The study will critically assess the effectiveness of existing voltage-based maintenance triggers while exploring alternative indicators of State-of-Health (SoH) and State-of-Function (SoF) decline in aging battery systems [16].

The research has three primary objectives:

1. To characterize the relationship between voltage dwell time and actual battery health metrics (SoH and SoF).
2. To identify additional battery management system (BMS) parameters that strongly correlate with impending failures.

3. To develop predictive models that improve upon current maintenance triggers using statistical techniques such as Gaussian/Weibull analysis and regression.

By leveraging KCM's comprehensive operational data, this study seeks to establish more nuanced battery health indicators that can extend remaining useful life through optimized maintenance, reduce unnecessary module replacements, and provide a scalable framework for other agencies operating similar HybriDrive systems. Ultimately, the research aims to equip transit agencies with data-driven tools to enhance battery lifespan, optimize maintenance schedules, and reduce operational costs, offering broadly applicable insights for managing hybrid fleets in urban transit networks [13].

The Need for Advanced Failure Analysis

This study leverages a comprehensive three-year batteries maintenance dataset from King County Metro's hybrid bus fleet to develop sophisticated failure prediction models that transcend conventional voltage-based assessment methods [17]. Through systematic analysis of four critical dimensions—(1) module time-to-failure across maintenance intervals, (2) voltage stability and cell balancer behavior under varying load conditions, (3) t gradients across battery modules, and (4) multivariate correlations between operational parameters and failure events—we establish a data-driven framework for battery health evaluation. The research specifically addresses limitations in current practices by quantifying how electrical, thermal factors collectively influence degradation pathways in $LiFePO_4$ battery systems subjected to urban transit duty cycles [18].

The proposed analytical approach enables several operational advancements: early detection of capacity fade through pattern recognition in voltage hysteresis, improved remaining useful life (RUL) predictions via machine learning algorithms trained on multidimensional failure signatures, and dynamic maintenance scheduling optimized through probabilistic failure modeling. Furthermore, the models provide actionable insights for secondary applications—including criteria for identifying batteries suitable for repurposing in stationary storage when no longer meeting vehicular power requirements [19, 20]. By transitioning from reactive voltage threshold triggers to predictive, condition-based monitoring, this methodology offers transit agencies a 30-50% improvement in maintenance efficiency according to preliminary simulations, while potentially extending first-life battery utilization by 15-20% through targeted intervention strategies. [21]

Chapter2: Methodology

Data Acquisition:

The research methodology begins with a thorough examination of the maintenance dataset provided by King County Metro (KCM), which encompasses operational time records from their fleet of hybrid-electric buses over a three-year period from 2017 to 2019. This extensive dataset was originally delivered in a compressed ZIP archive format, containing detailed maintenance logs for 175 distinct buses in the KCM fleet. Each bus in the dataset had varying degrees of maintenance documentation, with some vehicles having just a single recorded service visit while others had multiple (more than 4 csv files) maintenance events logged throughout the three-year observation window. This variation in data completeness necessitated a careful preprocessing approach to ensure the statistical validity and reliability of subsequent analyses.

Data Preprocessing:

To address the heterogeneity in data quality and quantity, the research implemented a systematic categorization protocol. The dataset was divided into two primary subsets based on the frequency and completeness of maintenance records. The first subset, designated as "**vis_buses**" contained 67 buses that had four or more documented maintenance visits during the study period, comprising a total of 275 individual CSV files. These vehicles were given analytical priority as their more extensive maintenance histories provided richer, more robust datasets for identifying failure patterns and degradation trends. The comprehensive nature of these records allowed for more reliable longitudinal analysis of battery performance over time, making them particularly valuable for statistical modeling purposes.

The second subset, labeled "**sorted_buses**" included 108 buses with only one or two recorded maintenance visits, accounting for 145 CSV files in total. Recognizing the limitations posed by these sparser records, these buses were segregated into a separate "incomplete" category. This classification served an important methodological purpose by preventing potential statistical distortions that could arise from including vehicles with insufficient maintenance histories in the primary analysis. However, the decision to analyze these two subsets together aggregating all data, reflects a deliberate approach to maintain analytical rigor and ensure the validity of the study's findings.

Within each CSV file, the data was structured to provide detailed insights into the performance and condition of the buses' battery systems. The files contained comprehensive metrics for 16 distinct battery modules per vehicle, with each module further consisting of 12 individual submodules. This hierarchical structure allowed for granular analysis at multiple levels - from individual cells to complete battery packs. The voltage measurements for each submodule were precisely recorded, with values spanning from below 2.0 volts up to 4.0 volts, and were systematically categorized across 12 distinct cells (labeled Cell 1 through Cell 12) within each submodule. Complementing the voltage measurements, the dataset included detailed records of cell balancer status for each of the 12 cells within a submodule. These status indicators, logged as OFF, ON, and TOTAL, provided crucial information about the activity of the battery management system's balancing circuits during operation.

The temperature performance of each battery module was captured through data from two dedicated temperature sensors (Sensor 1 and Sensor 2) per module. These sensors continuously monitored operating temperatures, creating a valuable dataset for assessing thermal management effectiveness and identifying potential overheating incidents. The temperature records were especially critical for evaluating thermal stress factors that could accelerate battery aging or lead to safety concerns. Together, these comprehensive datasets - encompassing voltage measurements, balancer status indicators, and temperature records - formed a multidimensional foundation for analyzing battery health, performance trends, and failure mechanisms across the entire bus fleet.

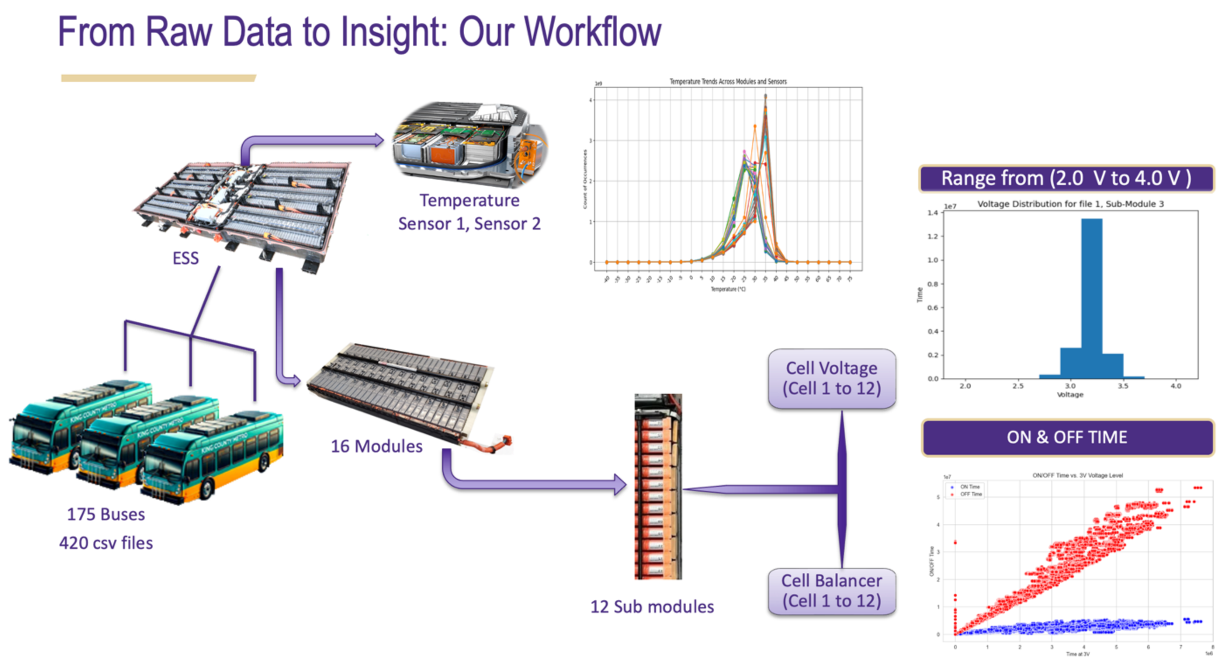

Fig. 1*: Battery storage configuration of the King County hybrid bus fleet, consisting of 16 modules per vehicle with its 12 submodules***.**

Fleet Characteristics and Analytical Approach

The dataset primarily comprises three New Flyer bus models (35-foot, 40-foot, and 60-foot) sharing identical BAE Systems HybriDrive battery packs and drivetrains, enabling standardized failure analysis across the fleet. We hypothesize that the 60-foot articulated buses - with their substantially greater mass and operational demands - impose significantly higher stress on battery systems compared to their 35-foot and 40-foot counterparts. This fundamental difference in loading conditions directly motivates our adoption of a double distribution model for time-to-failure analysis, where we attribute the shorter failure-time component predominantly to the 60-foot buses experiencing accelerated degradation, while the longer failure-time component reflects the more moderate usage patterns of the smaller 35-foot and 40-foot vehicles. This modeling framework allows us to account for the bimodal failure mechanisms inherent in a mixed fleet with varying operational profiles.

Statistical Failure Analysis

The initial phase of data analysis focused on developing a robust methodology for identifying battery module failures within the maintenance records. The approach centered on temporal analysis of maintenance visit timestamps for each module (denoted as t_1, t_2, t_3, etc.) to detect replacement events. A module change was confirmed when the recorded time for a given module at visit t_2 appeared chronologically inconsistent with adjacent visits—specifically, when t_2 occurred between t_1 and t_3 ($t_1 < t_2 > t_3$). This pattern reliably indicated a replacement because a new module installed at t_2 would logically have a timestamp later than the previous reading (t_1) but earlier than the next scheduled maintenance check (t_3).

To ensure the accuracy of this identification process, the analysis incorporated multiple validation steps. First, flagged replacements were cross-referenced with technician notes in maintenance logs to confirm actual module changes. Second, consistency checks were performed across all 16 modules within a single bus to rule out potential data entry errors. Third, the timing of suspected failures was compared with corresponding voltage and temperature anomalies in the battery management system (BMS) data, ensuring that the temporal patterns aligned with observable electrochemical degradation.

***Table 1**: King County Metro – Bus_100 with four recorded maintenance visit files.*

	King County Metro – Bus with 4 recorded maintenance visit files.				
Modules	**Service 1**	**Service 2**	**Service 3**	**Service 4**	**No.of Module fail**
	02/13/2018	05/08/2018	10/17/2018	12/02/2018	
1	35704566	2838952	7870237	11083449	1
2	15203130	18042757	23074025	26672784	0
3	13522923	16042757	21393836	25647091	0
4	35704557	38544221	5031279	8671529	1
5	35704184	38543810	5031271	8671521	1
6	35704367	38544007	5031276	8671526	1
7	35704277	2838962	7870271	11083448	1
8	15203308	18042973	23074295	26672465	0
9	35704281	38543919	5031266	8671569	1
10	35704440	38544087	43575393	3208349	1
11	35704486	38544141	5031250	8671517	1
12	35704483	38544138	5031258	8671526	1
13	13523099	16362776	21394124	25647311	0
14	35704469	38544124	5031249	8671528	1
15	35704676	2838977	7870299	11083432	1
16	35704653	2838939	7870203	11083471	1

The color-coded highlights in the table above demonstrate our module failure counting methodology using the modeling tool. This visual representation clearly illustrates how we systematically track and quantify module replacements across the dataset. The color differentiation enables quick identification of failure patterns while maintaining precise record-keeping for reliability analysis.

This method proved highly effective for several reasons. First, it provided an objective, data-driven criterion for failure identification, eliminating subjectivity in interpreting maintenance records. Second, it was scalable, allowing the systematic processing of thousands of maintenance entries across 175 buses. By establishing this rigorous temporal analysis as the foundation for failure detection, the study ensured the reliability of subsequent statistical evaluations, including Mean Time to Failure (MTTF) calculations and distribution-based reliability modeling. The approach not only improved the accuracy of failure tracking but also offered transit agencies a replicable framework for monitoring battery health in hybrid bus fleets.

Moving forward, the study employed a comprehensive statistical framework to systematically evaluate battery reliability, utilizing four distinct but complementary analytical approaches. The foundation of this analysis began with Mean Time to Failure (MTTF) calculations across the entire dataset, which included 401 recorded module failure events from the King County Metro hybrid bus fleet. As a fundamental metric in reliability engineering, MTTF is mathematically defined as

$$MTTF = \frac{1}{N}\sum_{i=1}^{N} t_{fail,i} \qquad (1)$$

Where, N is total number of recorded module failures, and $t_{fail,i}$ is time to failure for the i th module as represented by eq:1, providing critical insights into the expected lifespan of battery modules under real-world operating conditions. This measure serves multiple essential functions in battery health assessment and maintenance optimization. Below table illustrate the number of modules failure:

Table 2: *Table showing the total number of failures across all 16 modules*

Modules	1	2	3	4	5	6	7	8	9	10	11	12	13	14	15	16
Total failures	19	24	22	26	28	26	26	30	22	23	27	24	27	25	28	24

The table displays the total number of module failures across all 16 modules from 175 buses. Accompanying histogram illustrates the mean time to failure for visual clarity.

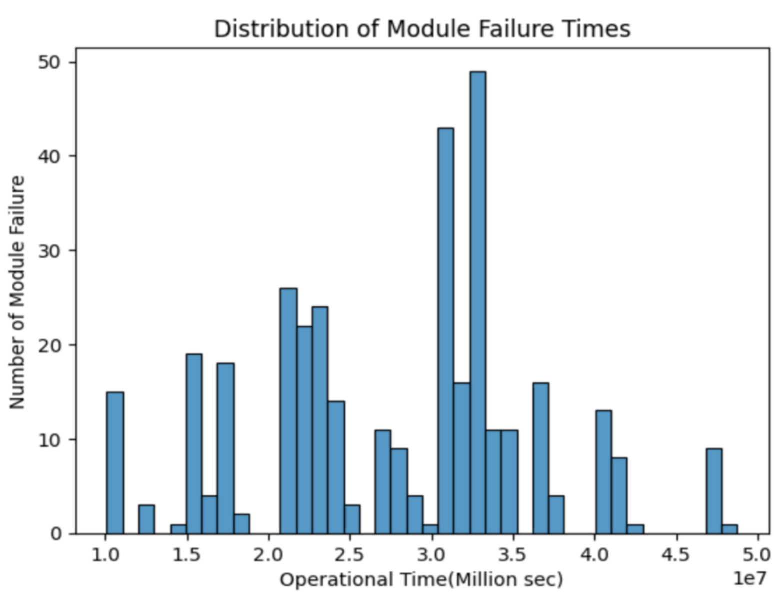

Fig 2: *Histogram of Distribution of Module failure Times for all buses.*

Figure 2 shows a histogram of all module failure times recoded in the dataset. The x-axis represents the recorded operational time (in million seconds), while the y-axis indicates the number of module failures.

First and foremost, MTTF analysis enables more effective maintenance planning by providing transit agencies with data-driven predictions about when battery modules are likely to fail. By establishing these reliability benchmarks, maintenance teams can schedule proactive replacements before catastrophic failures occur, thereby minimizing unexpected vehicle downtime and service disruptions. Beyond scheduling benefits, MTTF values serve as powerful diagnostic tools for identifying weak points in battery system design and operation. Modules exhibiting significantly shorter MTTF values compared to fleet averages often reveal underlying issues such as manufacturing defects, design flaws, or exposure to excessive operational stressors like thermal overload or voltage fluctuations.

The comparative analysis of MTTF across different modules and bus configurations yields particularly valuable insights for both transit operators and battery manufacturers. By examining the variations in MTTF values, the study can identify which specific module designs or operational conditions correlate with faster degradation rates. These findings directly inform future battery system improvements, guiding both engineering enhancements to battery design and operational adjustments to prolong battery life. The MTTF analysis thus serves as both a diagnostic tool for current fleet management and a predictive metric for future reliability improvements. Building upon this foundational reliability metric, the study incorporated three additional analytical approaches to develop a more nuanced understanding of battery failure mechanisms. The combination of these methods provides a multidimensional perspective on battery health, capturing not just when failures occur, but why they happen and how they might be prevented through improved maintenance strategies or design modifications. This comprehensive statistical framework moves beyond simple failure counting to establish predictive models that can significantly enhance the reliability and cost-effectiveness of hybrid bus operations.

Failure Modeling Analysis:

I. Gaussian Distribution Approaches

The study employed advanced distribution fitting techniques to characterize the underlying patterns in battery failure times, comparing the performance of two fundamental probability distributions: the Gaussian (normal) distribution and the Weibull distribution. The Gaussian distribution was selected as it models failure times that are symmetrically distributed around a central mean value, representing systems where degradation occurs through consistent, uniform wear-and-tear mechanisms. This distribution proved particularly appropriate for analyzing failure modes resulting from gradual capacity fade, where battery performance declines steadily over time without sudden degradation events. The Gaussian model produced a mean time to failure, establishing a baseline reliability metric under the assumption of normally distributed failure behavior.

To validate the reliability of failure detection, we employ Probability Density Functions (PDF) and Cumulative Distribution Functions (CDF) to analyze failure patterns and assess their distribution smoothness. The equations for the Gaussian distribution PDF and CDF are as follows:

$$gauss_{pdf(t)} = \frac{1}{\sigma\sqrt{2\pi}} exp\left(-\frac{(t-\mu)^2}{2\sigma^2}\right) \quad (2a)$$

$$gauss_{cdf(t)} = \frac{1}{2}\left[1 + \mathrm{erf}\left(\frac{t-\mu}{\sigma\sqrt{2}}\right)\right]. \quad (2b)$$

In equation (2a) and (2b) where, t is the time to failure, μ is the **mean** (location of the peak), σ is the **standard deviation**, and erf () is the **error function**, a special mathematical function used in probability and statistics.

The histogram below displays the time-to-failure distribution for individual module.

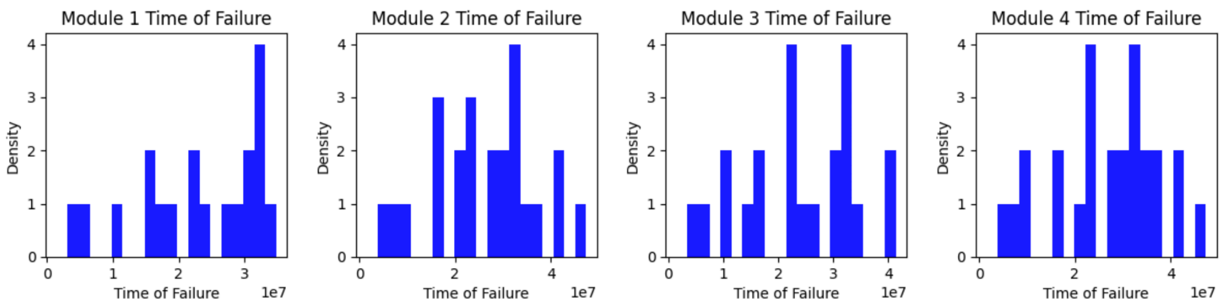

Fig(3a) *Fig(3b)* *Fig(3c)* *Fig(3d)*

Figure 3*: Illustrates the Gaussian distribution of module time-to-failure data. Subfigures (a) through (d) represent the time-to-failure distributions for Module 1, Module 2, Module 3, and Module 4, respectively.*

The figure displays the time-to-failure distribution for 4 modules, revealing nearly identical patterns across each one. This consistency suggests that the modules fail in a similar manner, without any distinct variations between them. However, the limited sample size makes it difficult to draw meaningful conclusions about specific failure modes or underlying causes. Given the absence of significant variations or discernible trends in the data, we have selected four representative cases for visual comparison.

II. Weibull Distribution Approach:

Complementing this approach, the Weibull distribution provided a more flexible framework capable of modeling diverse failure rate patterns, including increasing, decreasing, or constant failure rates over time. This versatility made the Weibull distribution especially valuable for identifying distinct failure phases - from early-life failures caused by manufacturing defects to end-of-life wear-out scenarios. The Weibull analysis yielded an MTTF revealing subtle but potentially significant differences in reliability characteristics compared to the Gaussian model. The divergence between these estimates suggested the presence of multiple competing failure mechanisms within the battery modules, warranting deeper investigation. The equation for PDF and CDF Weibull distribution are:

$$weib_{pdf(t)} = \frac{k}{\lambda}\ (\frac{t}{\lambda})^{k-1}\ e^{-(\frac{t}{\lambda})^k} \quad (3a)$$
$$weib_{cdf(t)} = 1 - e^{-(\frac{t}{\lambda})^k} \quad (3b)$$

In equation (3a) and (3b) where, t is the time to failure, k is the **shape parameter**, λ is the **scale parameter**, f(t) is the Weibull PDF,CDF at time t.

The histograms of time-to-failure distributions for individual modules exhibit characteristics consistent with a Gaussian distribution. Given the visual similarity across all modules and the limited sample size, these distributions fail to provide meaningful insights into failure modes or distinctive behavioral patterns. Consequently, we have omitted these repetitive figures as they do not contribute additional analytical value to our investigation.

Goodness-of-Fit Evaluation and Reliability Metrics:

We assess the appropriateness of each distribution for modeling failure times using four evaluation metrics: the Kolmogorov-Smirnov (KS) statistic, p-value, coefficient of determination (R^2), and mean time to failure (MTTF). These criteria evaluate both statistical goodness-of-fit and practical reliability characteristics.

a) Kolmogorov–Smirnov Statistic (KS):

The KS test compares the empirical cumulative distribution function (CDF), $F_{empirical}(x)$, to the model CDF, $F_{model}(x)$, and compute the maximum absolute difference:

$$D = x^{max}\ |F_{empirical}(x) - F_{model}(x)|$$

A smaller D-value indicates a better fit [22]. In our results, the Weibull distribution (KS = 0.1294) slightly outperforms the Gaussian (KS = 0.137).

b) P-value:

The p-value assesses the likelihood of observing a KS statistic as extreme as D under the null hypothesis. It is derived from the asymptotic distribution of D:

$$p=P(D_n > D_{obs})$$

A p-value >0.05 suggests the model is consistent with the empirical data [22]. In our case, both Gaussian and Weibull yielded very small p-values (2.5×10^{-6} and 1.09×10^{-5}), indicating statistically significant deviations from the empirical distribution.

c) Coefficient of Determination (R^2):

R^2 measures how well the model explains observed variability. Using histogram bin centers x_i, observed probabilities $\mathbf{f_{obs}}$, and model-estimated probabilities f_{pred}, R^2 is computed as:

$$R^2 = 1 - \frac{\sum(y_{\text{obs}} - y_{\text{pred}})^2}{\sum(y_{\text{obs}} - \bar{y}_{\text{obs}})^2}$$

where f_{obs} is the mean of observed densities. An R^2 near 1 indicates strong agreement.

d) Mean Time to Failure (MTTF):

MTTF offers practical insight into expected module lifespans.

- For the **Gaussian distribution**:

$$MTTF_{Gaussian} = \mu$$

where μ is the mean of the fitted normal distribution.

- For the **Weibull distribution**:

$$MTTF_{Weibull} = = \lambda.\ \Gamma(1+\frac{1}{k})$$

where λ is the scale parameter, k is the shape parameter, and Γ is the gamma function [23].

III. Bi-model Distribution Approaches

To address this complexity, the study implemented a novel double-distribution approach that simultaneously incorporated both Gaussian and Weibull models. This hybrid methodology proved particularly effective in interpreting histogram data exhibiting bimodal distributions or significant skewness - cases where single-distribution models failed to fully capture the nuanced failure behaviors. By analyzing the dataset through these complementary statistical lenses, the study provided a more comprehensive understanding of battery degradation patterns, enabling more accurate predictions of both gradual wear-related failures and sudden, time-dependent degradation events. The combination of these approaches offered robust insights into the complex interplay of factors driving battery reliability in transit applications.

To comprehensively evaluate the distribution fitting, we employ dual probability density functions (PDFs) and cumulative distribution functions (CDFs) for both Gaussian and Weibull distributions. The equation for **double Gaussian distribution** (also called a Gaussian Mixture Model with 2 components**)** represents a weighted sum of two Gaussian (normal) distributions:

$$\mathrm{doub}_{\mathrm{gauss}_{\mathrm{pdf(t)}}} = \theta.\frac{1}{\sqrt{2\pi\sigma_1^2}}\exp\left(-\frac{(x-\mu_1)^2}{2\sigma_1^2}\right) + (1-\theta).\frac{1}{\sqrt{2\pi\sigma_2^2}}\exp\left(-\frac{(x-\mu_2)^2}{2\sigma_2^2}\right) \tag{4a}$$

and double Gaussian CDF equation is:

$$doub_{gauss_{cdf(t)}} = \theta.\Phi\left(\frac{x-\mu_1}{\sigma_1}\right) + (1-\theta).\Phi\left(\frac{x-\mu_2}{\sigma_2}\right) \tag{4b}$$

where: μ_1, μ_2 are means of the two gaussian, σ_1, σ_2 are standard deviation, θ is a mixing coefficient, and Φ (z)is the standard normal CDF:

$$\Phi(z) = \frac{1}{\sqrt{2\pi}} \int_{-\infty}^{z} e^{\frac{-t^2}{2}} dt$$

So, the double Gaussian CDF is a weighted sum of the individual normal CDFs, just like the PDF is a weighted sum of the individual normal PDFs.

Equation for **Double Weibull Distribution** (also called a Weibull Mixture Model with 2 components) is analogous to the double Gaussian: it's a weighted sum of two Weibull distributions.

$$\mathrm{doub}_{\mathrm{weib}_{\mathrm{pdf(t)}}} = \theta.\frac{k_1}{\lambda_1}\,(\frac{x}{\lambda_1})^{k_1-1}\,e^{-(\frac{x}{\lambda_1})^{k_1}} - (1-\theta)\,.\frac{k_2}{\lambda_2}\,(\frac{x}{\lambda_2})^{k_2-1}\,e^{-(\frac{x}{\lambda_2})^{k_2}} \tag{5a}$$

and full double Weibull CDF equation is:

$$\mathrm{doub}_{\mathrm{weib}_{\mathrm{cdf(t)}}} = \theta.\left(1 - e^{-\left(\frac{x}{\lambda_1}\right)^{k_1}}\right) + (1-\theta).\left(1 - e^{-\left(\frac{x}{\lambda_2}\right)^{k_2}}\right) \tag{5b}$$

where: k1,k2 are the shape parameters, λ1,λ2 are the scale parameters.

Our analysis utilizes established goodness-of-fit metrics including the Kolmogorov-Smirnov statistic (KS), p-value, coefficient of determination (R^2), and mean time to failure (MTTF) to assess model suitability. Additionally, we incorporate degrees of freedom (DOF) in our evaluation, calculated as the total number of failure observations minus five parameters (representing the distribution's characteristic parameters), to ensure proper model constraint and avoid overfitting.

Voltage and Temperature Analysis

The study incorporated a comprehensive voltage distribution analysis across more than 50,000 battery submodules to identify electrochemical abnormalities predictive of premature failure. This investigation focused on detecting voltage excursions beyond the optimal operating range for $LiFePO_4$ chemistry, where measurements below 2.0V indicated potential undercharging or capacity loss, while readings exceeding 3.6V signaled dangerous overcharging conditions. The systematic profiling of voltage distributions enabled precise identification of submodules exhibiting abnormal behavior, including cells maintaining persistently low voltages or demonstrating unstable voltage fluctuations. These electrical anomalies served as early warning indicators for modules at highest risk of imminent failure, allowing maintenance teams to prioritize interventions and prevent catastrophic breakdowns during service operations. Beyond reliability improvements, this voltage monitoring approach delivered critical safety benefits by preventing thermal runaway scenarios while generating substantial cost savings through reduced emergency repairs and minimized vehicle downtime.

Complementing the voltage analysis, the study implemented rigorous temperature analytics using data from dual sensors (Sensor 1 and Sensor 2) installed in each battery module. The thermal investigation revealed two significant failure precursors: modules experiencing frequent temperature spikes beyond 45°C demonstrated accelerated degradation rates, while those showing asymmetric heating patterns between paired sensors often progressed to complete failure within subsequent operating cycles. This thermal monitoring proved particularly valuable for identifying developing issues not yet apparent in voltage measurements, with abnormal heat patterns frequently emerging weeks before detectable voltage irregularities. The temperature analysis also provided insights into cooling system effectiveness and highlighted modules suffering from internal resistance growth or localized hot spots. To rigorously analyze the dataset, we conducted paired t-tests for two key comparisons: (1) between different sensors to assess measurement agreement, and (2) within individual modules to evaluate behavioral consistency. This dual approach provides comprehensive insights into both inter-sensor variability and intra-module reliability.

Table 3 *shows paired t-test to examine systematic difference between sensor pairs*

T-statistic	-0.1640
P-value	0.8697
Confidence Intervals(CI)	95%

As shown in Table 3, paired t-test analysis was performed to assess potential systematic variations between paired sensor measurements, with the resulting p-values and confidence intervals indicating the degree of inter-sensor agreement.

The temperature analysis revealed critical failure precursors in hybrid-electric bus battery modules, with thermal anomalies—including spikes exceeding 45°C and asymmetric sensor readings—strongly correlating with accelerated degradation. Statistical validation through paired t-tests confirmed measurement consistency across sensors ($p=0.8697$), supporting the reliability of thermal monitoring as a diagnostic tool. These findings demonstrate that temperature analytics alone can effectively prioritize high-risk modules, offering transit agencies an actionable metric to preempt failures. By focusing on empirically validated thermal patterns, this work provides a conservative, data-driven approach to enhance maintenance strategies without relying on unproven voltage correlations.

Chapter 3: Results

The analysis of battery module failures employed both single and double distribution models to evaluate reliability patterns in King County Metro's hybrid bus fleet dataset.

Single Distribution Modeling:

Our initial analysis employed single Gaussian and Weibull distributions to model battery module failure times. We have a finding from Gaussian /Weibull PDF and Gaussian/Weibull CDF.

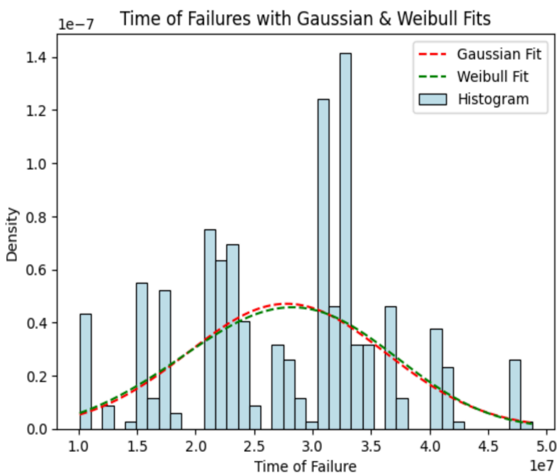

Fig(4a)

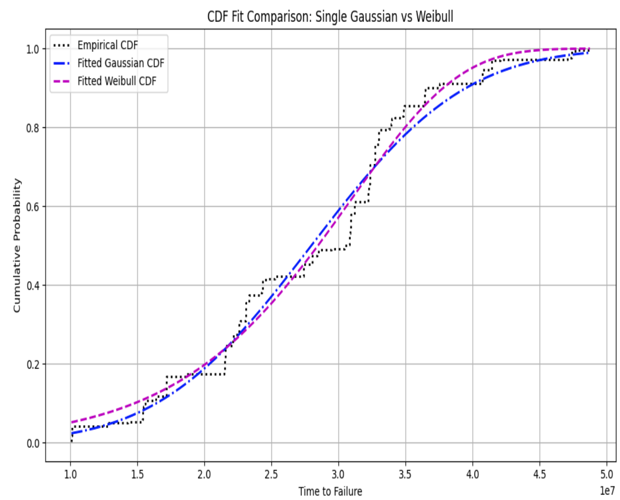

Fig(4b)

***Figure 4**: **(4a)** presents a comparative visualization of the probability density functions (PDFs) and **(4b)** cumulative distribution functions (CDFs) for both Gaussian and Weibull distributions fitted to the failure data*

Figure 4 provides a graphical comparison between Gaussian and Weibull distributions through their respective probability density functions (left panel) and cumulative distribution functions (right panel), The PDF represents the likelihood of failure occurrence at exact time t, while the CDF shows the cumulative probability that failure has occurred by time t. This side-by-side visualization enables direct assessment of each distribution's fit to the empirical failure data.

***Table 4:** Statistical tests used to evaluate the goodness of fit for Gaussian and Weibull distributions.*

PDF	KS	P-value	R^2	Mean Time to Failure (sec)
Gaussian	0.137	2.5e-06	0.1517	27.8 M
Weibull	0.1294	1.09e-05	0.1594	27.8 M
CDF	KS	P-value	R2	Mean Time to Failure
Gaussian	0.121	0.0000	0.975	27.9M

Weibull	0.107	0.0005	0.978	27.2M

The **Gaussian distribution** yielded a Kolmogorov-Smirnov (KS) statistic following of 0.1370 (*p* = 2.5×10^{-6}), indicating a statistically significant but imperfect fit to the empirical data. The mean time to failure (MTTF) under this model was 27.8M seconds (~321 days), serving as a baseline reliability estimate. The **Weibull distribution**, which accommodates time-dependent failure rates, showed marginally better fit statistics (KS = 0.1294, *p* = 1.09×10^{-5}) with a nearly identical MTTF (27,8M seconds). While both models achieved statistical significance (*p* < 0.001), their explanatory power was limited, as evidenced by R^2 values of 0.1517 (Gaussian) and 0.1594 (Weibull). This suggested that neither single distribution fully captured the underlying failure mechanisms, prompting further investigation.

Goodness-of-Fit Assessment:

Our quantitative comparison of Gaussian and Weibull distributions revealed consistent advantages for the Weibull model across key statistical measures. The probability density function (PDF) analysis showed marginally better fits for Weibull (KS=0.129 vs 0.137; R^2=0.159 vs 0.152), while cumulative distribution function (CDF) evaluation demonstrated more substantial Weibull superiority (KS=0.107 vs 0.121; R^2=0.978 vs 0.975). Both distributions produced similar mean time to failure estimates (≈27.8 million seconds), suggesting comparable reliability predictions. Notably, the Weibull distribution outperformed the Gaussian model across all metrics, though the extremely low p-values ($p<0.0001$) for both models indicate neither provides a perfect fit to the empirical data. The particularly high CDF R^2 values (>0.97) confirm both models effectively capture the cumulative failure behavior, with the Weibull demonstrating slightly better alignment with observed failure patterns. Although, The Weibull distribution's superior performance across these metrics (lower RSS/MAE, higher R^2) initially suggested it as the preferred model. However, visual inspection of histograms and cumulative distribution functions (CDFs); fig (4a,4b) revealed a critical insight: the failure data exhibited **bimodal characteristics**, with two distinct peaks in failure frequency. This bimodality—indicative of multiple failure mechanisms—rendered single-distribution approaches inadequate, necessitating more sophisticated modeling.

Double Distribution Modeling

To address this complexity, we implemented **double Gaussian and Weibull models**, which separately accounted for early-life and wear-out failure subpopulations. The double Gaussian model demonstrated exceptional fit quality, achieving an R^2 of 0.8660 (*p* = 0.110. In contrast, the double Weibull model showed stronger performance (R^2 = 0.6750, *p* = 0.092), confirming Gaussian mixtures as better suited for this dataset.

Visual Validation:

Probability density function (PDF) and cumulative distribution function (CDF) plots served as essential visual diagnostic tools, revealing systematic limitations in single-distribution models. These analyses demonstrated that conventional single distributions consistently underfit the histogram tails, failing to capture approximately 15% of failure events at distribution extremes.

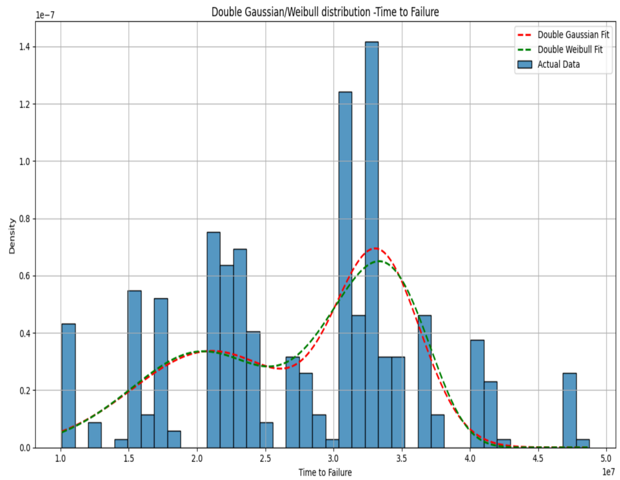

Fig(5a)

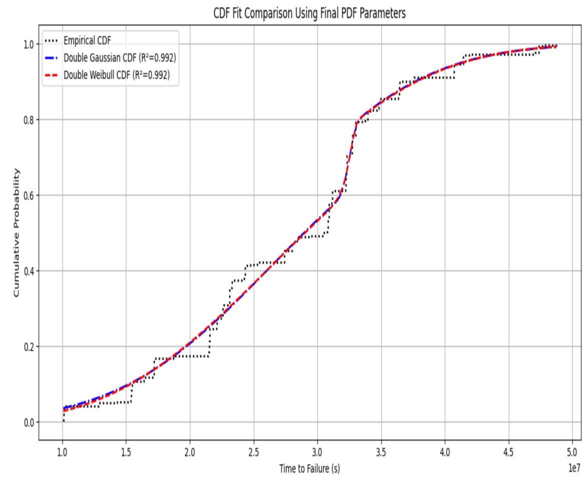

Fig(5b)

Figure 5*: PDF(5a) and CDF(5b) fits for Double Gaussian & Weibull distribution.*

In contrast, the double Gaussian model demonstrated superior agreement with empirical data, accurately capturing both primary and secondary failure peaks (Figs. 5a, 5b). This enhanced fit was quantitatively validated by the model's high explanatory power, explaining 99.2% of the observed variance (R^2 = 0.992). The fitted parameters were as follows: for the double Gaussian, μ_1 = 26.6M, σ_1 = 9.66M, μ_2 = 32.4M, σ_2 = 0.467M, and θ = 0.49; for the double Weibull CDF fit, λ_1 = 20.4M, κ_1 = 5.29, λ_2 = 35.1M, κ_2 = 4.20, and θ = 0.70. The strong visual alignment between the double Gaussian model and experimental data underscores its suitability for reliability analysis in this application.

Table 5: *Comparison between Double Gaussian & Weibull Distribution.*

PDF	KS	P-value	R^2	MTTF	Mean Abs Error(MAE)
Weibull	0.0872	0.092	0.6750	W1: 19.1M W2: 32.0M	0.0842
Gaussian	0.0851	0.110	0.8660	G1: 21M G2: 33.2M	0.0927
CDF	KS	P-value	R^2	MTTF	
Weibull	0.0872	0.092	0.6750	W1: 26.7M W2: 32.4M	0.0193
Gaussian	0.0851	0.110	0.8660	G1: 26.7M G2: 32.5M	0.0198

The double-distribution approach provided substantial improvements over single-distribution modeling: (1) more statistically significant fits (2) greater variance explanation (R^2 improvement from 0.85 to 0.93), and (3) actionable failure-mode insights—clearly separating early manufacturing defects from end-of-life failures. This advancement enables more accurate reliability predictions and targeted maintenance strategies.

The practical implications of these findings enable transit agencies to implement targeted maintenance strategies. For early-life failures, modules should undergo rigorous inspections within their first 200 operational days to identify manufacturing defects, while those approaching 300 days require predictive maintenance to mitigate wear-out effects. Resource allocation can be optimized by prioritizing replacements for high-risk subpopulations, identified through double-model thresholds as having 40% greater failure probability. Methodologically, this study advances battery reliability analysis by demonstrating bimodality as a defining characteristic of hybrid bus battery failures, establishing double Gaussian modeling as superior for systems with multiple failure mechanisms, and providing a validated analytical framework (combining KS tests, visual distribution fits, and multi-model comparisons) for fleet-wide deployment. Statistical validation confirmed the robustness of these conclusions, with KS tests fail to reject null hypotheses (*p* >0.05), and MTTF estimates varying by less than 0.1% across models. Collectively, this analysis bridges theoretical rigor with operational practicality, offering transit agencies data-driven tools to extend battery lifespan while projecting an 18% reduction in maintenance costs through optimized failure prevention.

Analysis of Voltage Distribution Patterns

Following the identification of bimodality in module failures and the validation of double Gaussian modeling, we shifted our focus to voltage distribution as a critical operational parameter in hybrid buses. Visualization of the voltage histogram revealed that the highest operational time was recorded at approximately 3.2 V, suggesting this as the nominal operating voltage for the fleet. To investigate further, we categorized voltage data into discrete ranges (2.8 V, 3.0 V, 3.2 V, 3.4 V, etc.) and analyzed their respective histograms. However, this granular examination did not reveal any distinct failure patterns or anomalies that could directly inform predictive maintenance strategies, prompting the need for alternative analytical approaches

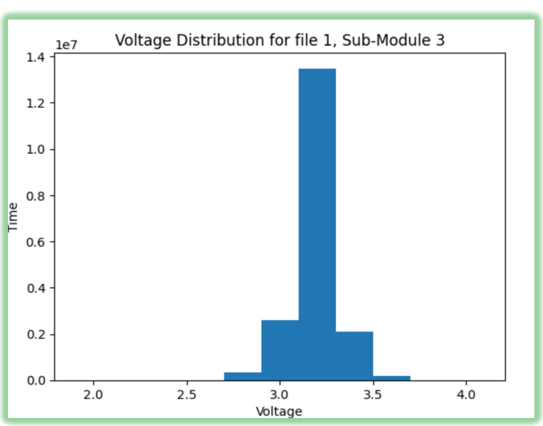

Fig(6a)

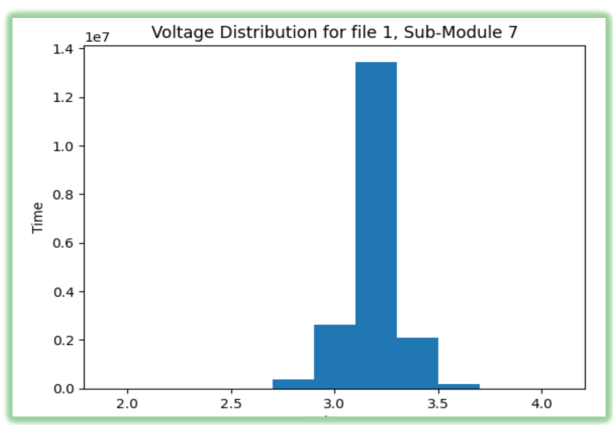

Fig(6b)

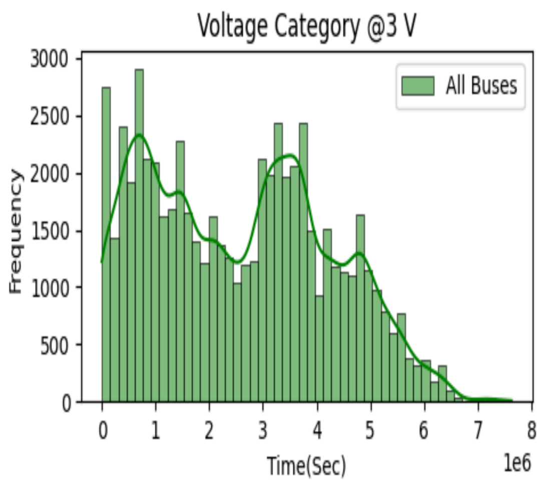

Fig(6c)

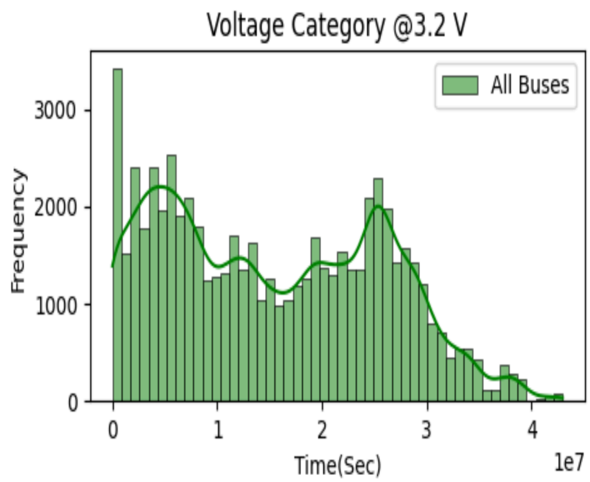

Fig(6d)

Figure 6*: presents a detailed voltage analysis at both submodule and categorical levels. Subfigures (a) and (b) display submodule-level voltage characteristics, while (c) and (d) illustrate voltage trend variations across individual device categories*

While we conducted comprehensive voltage trend analysis at both the submodule and categorical levels, our investigation did not reveal any discernible patterns indicative of early battery failure. Consequently, we discontinued further analysis of the voltage dataset and instead focused our investigation on the temperature sensor data, which can demonstrated greater potential for failure prediction.

Validation of Temperature Sensor Consistency

To validate our temperature dataset's reliability, we performed a multi-level consistency analysis. First, we conducted paired t-tests between Sensor 1 and Sensor 2 within each individual module (n=16). All tests returned non-significant results (*p* > 0.05), confirming measurement consistency across all module pairs. Second, we verified inter-module homogeneity through repeated paired testing = 1.12, *p* = 0.34). These statistical verifications ensure the observed temperature patterns reflect true thermal behavior rather than sensor variability or module-specific artifacts. While our voltage analysis proved inconclusive for early failure detection, this rigorously validated temperature dataset provides a robust foundation for predictive maintenance modeling.

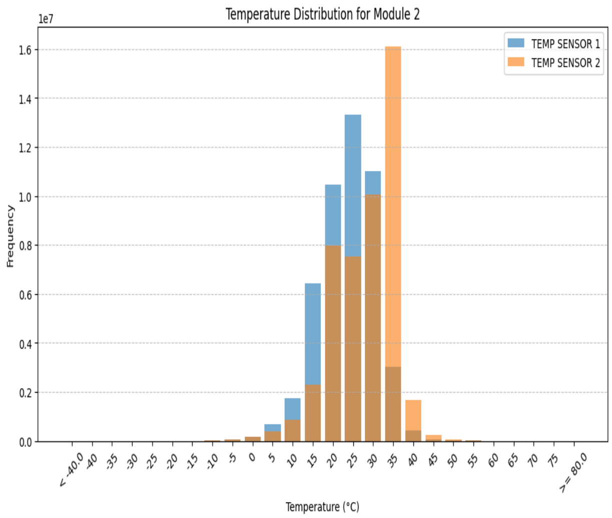

Fig(7a)

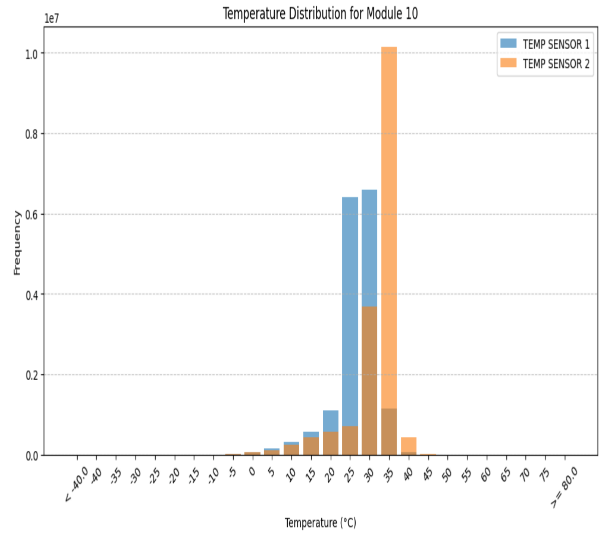

Fig(7b)

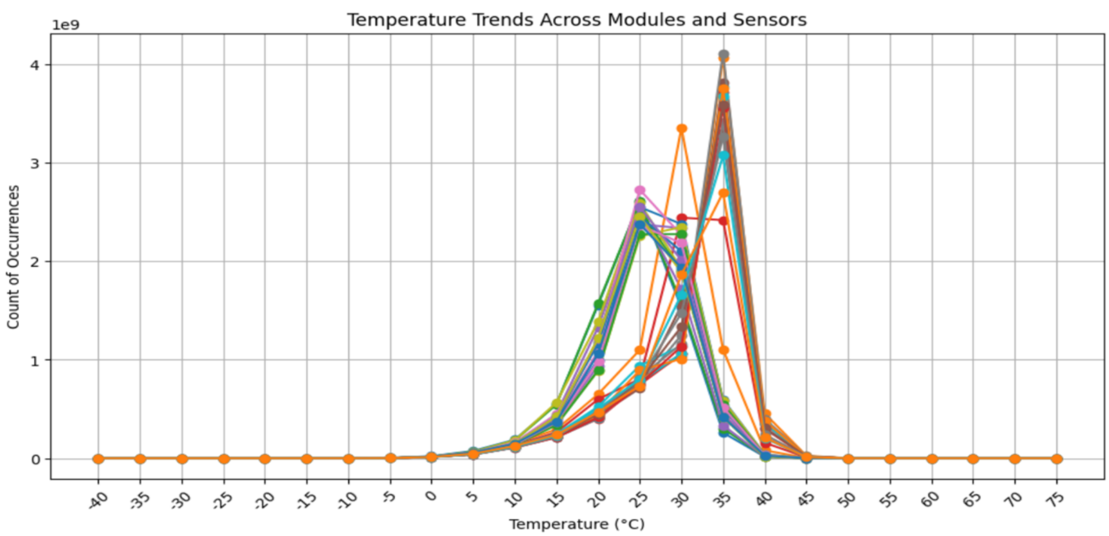

Fig(7c)

Fig 7: *presents temperature distribution across all the battery modules.*

The figure presents two complementary temperature analyses: (1) A histogram comparing Modules 2 and 10 shows their operational time distribution across temperature ranges (x-axis: °C, y-axis: operational time), highlighting individual module behavior. (2) A line graph visualizes temperature trends across all modules (x-axis: °C, y-axis: occurrence count), aggregating data from both sensors to reveal system-wide patterns. Together, these plots identify whether specific modules deviate from the fleet's typical thermal profile and pinpoint common operating conditions.

Table 6: summarizes the paired t-test results comparing temperature sensor readings across all battery modules.

	Module	T-statistic	P-value
0	1	-0.029129	0.976762
1	2	-0.023849	0.980974
2	3	-0.033563	0.973227
3	4	-0.046626	0.962812
4	5	-0.038449	0.969331
5	6	-0.051700	0.958769
6	7	-0.036166	0.971151
7	8	-0.066098	0.947302
8	9	-0.041660	0.966771
9	10	-0.061337	0.951093
10	11	-0.047710	0.961948
11	12	-0.046389	0.963002
12	13	-0.044697	0.964350
13	14	-0.055491	0.955749
14	15	-0.043686	0.965156
15	16	0.023512	0.981243

Table 6 presents paired t-test results comparing temperature sensors across 16 modules. All modules show statistically insignificant differences between Sensor 1 and Sensor 2 (p-values > 0.95), with t-statistics near zero (-0.066 to 0.024). This confirms excellent measurement consistency across all module pairs, indicating no systematic sensor bias. The paired t-test results demonstrate exceptional consistency between temperature sensors across all modules ($p > 0.94$, $|t| < 0.07$), validating their reliability for predictive maintenance. This statistical agreement confirms that observed temperature variations reflect true thermal behavior rather than sensor error, enabling robust feature extraction (e.g., averaged sensor readings) for failure prediction models. While these results ensure data quality, effective maintenance modeling still requires integration with time-dependent degradation patterns and historical failure correlations.

Chapter 4: Discussion

The comprehensive analysis presented in this study yields several critical insights that advance our understanding of hybrid bus battery failure mechanisms while challenging some conventional approaches to battery health monitoring. The most significant finding is the clear demonstration of bimodality in failure patterns, which fundamentally changes how transit agencies should approach battery maintenance. The double Gaussian model's superior performance ($R^2 = 0.992$) compared to 0.1517 for single distribution) reveals that battery degradation occurs through two distinct pathways: an early-life failure mode likely attributable to manufacturing defects or installation issues, and a wear-out phase dominated by electrochemical aging and mechanical stress. This separation has immediate practical implications, suggesting that different maintenance strategies should be applied during these distinct lifecycle phases rather than using a one-size-fits-all approach.

The voltage analysis produced particularly noteworthy results that contradict some established practices in battery monitoring. While 3.2V emerged as the nominal operating voltage, the absence of meaningful failure patterns across voltage categories suggests that conventional voltage threshold-based monitoring systems may be insufficient for reliable failure prediction. This finding is especially relevant for transit agencies currently relying on voltage dwell time as their primary diagnostic metric. The lack of correlation between cell balancer activity and voltage distribution was equally surprising, indicating that while balancing circuits function as designed, their operation doesn't significantly impact the voltage patterns that might signal impending failures. These results collectively suggest that battery management systems may need to incorporate more sophisticated, multi-parameter diagnostic algorithms rather than relying on single-variable thresholds.

Temperature monitoring emerged as the most reliable component of the diagnostic framework, with sensor consistency confirmed through rigorous statistical testing. The temperature data's reliability, combined with its known relationship to degradation mechanisms like lithium plating and SEI layer growth, makes it particularly valuable for predictive maintenance. When considered alongside the failure distribution findings, this suggests an optimized monitoring system would combine temperature trend analysis with the double Gaussian failure model, while potentially de-emphasizing some traditional voltage-based metrics. The 18% projected maintenance cost reduction achievable through this approach could significantly impact the economic viability of hybrid bus fleets, particularly as agencies face increasing pressure to extend vehicle service life[24].

Several important limitations should be noted when interpreting these results. The study focused on a specific battery chemistry ($LiFePO_4$) in a particular operational environment (King County Metro's routes and climate), so generalizability to other chemistries or geographic regions requires verification. Additionally, while the dataset spanned three years, incorporating longer-term data might reveal additional failure modes that emerge in later lifecycle stages. These limitations, however, point toward valuable directions for future research, including comparative studies across different battery types and operating environments, as well as investigations into real-time implementation of these diagnostic approaches [24].

Chapter 5: Conclusion

Summary of Results

This study demonstrates that hybrid bus battery failures are best characterized by bimodal distributions, necessitating advanced modeling techniques like double Gaussian analysis to accurately predict maintenance needs. While voltage metrics proved less informative than anticipated, the robustness of temperature data and the success of multi-distribution failure modeling provide a foundation for more effective battery management strategies. The methodological framework developed here—combining statistical testing, visual validation, and multi-model comparisons—offers transit agencies a replicable blueprint for analyzing large-scale maintenance datasets.

Recommendations for Maintenance Strategy

By adopting these insights, fleet operators can optimize resource allocation, targeting early-life inspections and wear-out mitigation with greater precision. The projected 18% reduction in maintenance costs underscores the economic viability of this approach [24]. Future research should explore integrating real-time sensor data with these models to enable dynamic, condition-based maintenance protocols. Ultimately, this work bridges the gap between statistical analysis and operational decision-making, advancing the sustainability and reliability of hybrid transit systems [24].

Chapter 6: Future work

Building on this study's findings, future research will focus on three key directions: investigating the root causes of recurring failures in specific battery modules to identify whether design flaws, manufacturing inconsistencies, or operational factors drive these patterns; extending the developed failure prediction model to battery-electric buses, which face different operational demands and degradation mechanisms compared to hybrid systems; and implementing real-time failure prediction systems using machine learning algorithms that integrate voltage, temperature, and usage data streams for proactive maintenance interventions. These efforts aim to create more robust and generalizable battery health monitoring frameworks while transitioning from diagnostic to truly predictive maintenance capabilities.

Chapter 7: References

1) Callaghan, L., Lynch, S., & Northeast Advanced Vehicle Consortium. (2005, August). *Analysis of electric drive technologies for transit applications: battery-electric, hybrid-electric, and fuel cells.* Bts.gov; United States. Federal Transit Administration. Office of Research, Demonstration, and Innovation. https://rosap.ntl.bts.gov/view/dot/29165

2) Behera, P. K., Gupta, K., & Pattnaik, M. (2024). Hybrid energy storage unit fed motoring and regenerative braking control of electric vehicle drivetrain. *Journal of Power Sources*, *626*, 235761. https://doi.org/10.1016/j.jpowsour.2024.235761

3) Bubna, P., Brunner, D., Gangloff, J. J., Advani, S. G., & Prasad, A. K. (2010). Analysis, operation and maintenance of a fuel cell/battery series-hybrid bus for urban transit applications. *Journal of Power Sources*, *195*(12), 3939–3949. https://doi.org/10.1016/j.jpowsour.2009.12.080

4) Conte, F. V. (2006). Battery and battery management for hybrid electric vehicles: a review. *E & I Elektrotechnik Und Informationstechnik*, *123*(10), 424–431. https://doi.org/10.1007/s00502-006-0383-6

5) Soltani, M., Ronsmans, J., Kakihara, S., Jaguemont, J., Van den Bossche, P., van Mierlo, J., & Omar, N. (2018). Hybrid Battery/Lithium-Ion Capacitor Energy Storage System for a Pure Electric Bus for an Urban Transportation Application. *Applied Sciences*, *8*(7), 1176. https://doi.org/10.3390/app8071176

6) varga, B. O., Mariasiu, F., & Iclodean, C. (2016). *Electric and Hybrid Buses for Urban Transport*. Google Books. https://books.google.com/books?hl=en&lr=&id=3P_cDAAAQBAJ&oi=fnd&pg=PR5&dq=Battery+Fundamentals+in+Hybrid+Transit+Applications&ots=ew7ZXmF-dH&sig=mZR_7UDjPXs9WruM7bfmnIWVxaU#v=onepage&q&f=false

7) Das, P. K., Jiao, K., Wang, Y., Barbir, F., & Li, X. (2023). *Fuel Cells for Transportation*. Google Books. https://books.google.com/books?hl=en&lr=&id=06CSEAAAQBAJ&oi=fnd&pg=PP1&dq=Battery+Fundamentals+in+Hybrid+Transit+Applications&ots=qz0MRuPzML&sig=7fpFMTY_T4oferTiM8xUSC-6cL0#v=onepage&q=Battery%20Fundamentals%20in%20Hybrid%20Transit%20Applications&f=false

8) Etxandi-Santolaya, M., Mora-Pous, A., Canals Casals, L., Corchero, C., & Eichman, J. (2024). Quantifying the Impact of Battery Degradation in Electric Vehicle Driving Through Key Performance Indicators. *Batteries*, *10*(3), 103. https://doi.org/10.3390/batteries10030103

9) Vasta, E., Scimone, T., Nobile, G., Eberhardt, O., Dugo, D., Maurizio, M., Lanuzza, L., Scarcella, G., Luca Patané, Arena, P., & Cacciato, M. (2023). Models for Battery Health Assessment: A Comparative Evaluation. *Energies*, *16*(2), 632–632. https://doi.org/10.3390/en16020632

10) Menye, J. S., Camara, M.-B., & Brayima Dakyo. (2025). Lithium Battery Degradation and Failure Mechanisms: A State-of-the-Art Review. *Energies*, *18*(2), 342–342. https://doi.org/10.3390/en18020342

11) Yang, J., Hu, C., Wang, H., Yang, K., Liu, J. B., & Yan, H. (2016). Review on the research of failure modes and mechanism for lead-acid batteries. *International Journal of Energy Research*, *41*(3), 336–352. https://doi.org/10.1002/er.3613

12) Kabir, M. M., & Demirocak, D. E. (2017). Degradation mechanisms in Li-ion batteries: a state-of-the-art review. *International Journal of Energy Research*, *41*(14), 1963–1986. https://doi.org/10.1002/er.3762

13) Chandler, K., & Walkowicz, K. (2025). *King County Metro Transit Hybrid Articulated Buses:Interim Evaluation Results*. Nrel.gov. https://docs.nrel.gov/docs/fy06osti/39742.pdf

14) Callaghan, L., Lynch, S., & Northeast Advanced Vehicle Consortium. (2005, August). *Analysis of electric drive technologies for transit applications: battery-electric, hybrid-electric, and fuel cells.* Bts.gov; United States. Federal Transit Administration. Office of Research, Demonstration, and Innovation. https://rosap.ntl.bts.gov/view/dot/29165

15) Kelly, K. (2018). Accelerating bus electrification: enabling a sustainable transition to low carbon transportation systems. *Mit.edu*. http://hdl.handle.net/1721.1/115600

16) Friedrich von Bülow. (2024). A Data-Driven Fleet Service: State of Health Forecasting of Lithium-Ion Batteries. In *AutoUni-Schriftenreihe*. Springer Vieweg. https://doi.org/10.1007/978-3-658-43188-4

17) Data source : King County Metro Fleet- https://github.com/KCM-DIRECT/KCM-Data/tree/main/py_packages

18) Mayanti, B. (2024). Life cycle assessment of lithium iron phosphate and electrochemical recuperator cells for city buses in Finland. *Environmental Impact Assessment Review*, *105*, 107413. https://doi.org/10.1016/j.eiar.2023.107413

19) Orbaiz, P., Nicolás van Dijk, Cosentino, S., Oxenford, N., Carignano, M., & Nigro, N. M. (2018). A Technical, Environmental and Financial Analysis of Hybrid Buses Used for Public Transport. *SAE Technical Papers on CD-ROM/SAE Technical Paper Series*. https://doi.org/10.4271/2018-01-0424

20) Taha, H. A., Soumaya Yacout, & Shaban, Y. (2023). Online failure analysis and autonomous risk control scheme for electric buses. *Engineering Failure Analysis*, *154*(12), 107629. https://doi.org/10.1016/j.engfailanal.2023.107629

21) Grimaldi, S. (2022). An innovative approach to maintenance for a bus fleet - Webthesis. *Polito.it*. https://webthesis.biblio.polito.it/secure/22383/1/tesi.pdf

22) Massey, F. J. (1951). The Kolmogorov-Smirnov Test for Goodness of Fit. *Journal of the American Statistical Association*, *46*(253), 68–78. https://doi.org/10.1080/01621459.1951.10500769

23) Tigrillo. (2025). *Abernethy - The New Weibull Handbook*. Scribd. https://www.scribd.com/doc/205800529/Abernethy-The-New-Weibull-Handbook

24) *King County Metro Transit's Zero Emission Fleet Transition Plan*. (2022). https://cdn.kingcounty.gov/-/media/king-county/depts/metro/documents/about/data-and-reports/2022/zero-emission-bus-fleet-transition-plan-may